Available online at www.sciencedirect.com

Journal of Organometallic Chemistry 671 (2003) 8–12

www.elsevier.com/locate/jorganchem

Short communication

Stereochemistry of mono- and dinuclear complexes of rhodium, iridium and ruthenium bearing bis(diphenylphosphinomethyl)phenylphosphine

Yosuke Kosaka [a], Yuichi Shinozaki [a], Yoshihiro Tsutsumi [a], Yoshihiro Kaburagi [a], Yasuhiro Yamamoto [a,*], Yusuke Sunada [b], Kazuyuki Tatsumi [b,1]

[a] *Faculty of Science, Department of Chemistry, Toho University, Miyama 2-2-1, Funabashi, Chiba 274-8510, Japan*

[b] *Department of Chemistry, Research Center for Materials Science, Graduate School of Science, Nagoya University, Furo-cho, Chikusa-ku, Nagoya 454-8602, Japan*

Received 17 December 2002; received in revised form 15 January 2003; accepted 21 January 2003

Abstract

Reaction of [Cp*MCl$_2$]$_2$ (**1a**: M = Rh and **1b**: M = Ir) or [(C$_6$Me$_6$)RuCl$_2$]$_2$ (**1c**) with bis(diphenylphosphinomethyl)phenylphosphine (dpmp) in the presence of KPF$_6$ generated mono- or dinuclear complexes [Cp*RhCl(dpmp)](PF$_6$) (**2a**), [(C$_6$Me$_6$)RuCl(dpmp)](PF$_6$) (**5c**), [Cp*MCl$_2$(dpmp)MClCp*](PF$_6$) (**3a**: M = Rh and **4b**: M = Ir) or [(C$_6$Me$_6$)RuCl$_2$(dpmp)RuCl(C$_6$Me$_6$)](PF$_6$) (**6c**), depending on reaction conditions. These complexes have two chiral centers and the diastereomers were separated and characterized by spectrometry and X-ray analyses. A diastereomer **2a**(**A**) was treated with AuCl(C$_4$H$_8$S), generating a hetero-tetranuclear complex [{Cp*RhCl$_2$(dpmp)Au}$_2$](PF$_6$)$_2$ (**7a**), whereas similar reactions of **5c** gave dinuclear complex [(C$_6$Me$_6$)RuCl(dpmp)AuCl](PF$_6$) (**8c**(**A**)).

Keywords: Pentamethylcyclopentadienyl(rhodium or iridium); (Arene)ruthenium; Bis(diphenylphosphinomethyl)phenylphosphine; Stereochemistry

Triphosphine, especially bis(diphenylphosphinomethyl)phenylphosphine (dpmp), plays an important role as backbone of the construction of polynuclear clusters. A review on its chemistry of rhodium, iridium and gold has been sited by Balch [1]. We have developed systematic syntheses of homo- and hetero-trimetallic platinum and palladium clusters with tridentate phosphine and isocyanide ligands [2]. These complexes are constructed fundamentally by square planar framework and contain dpmp, carbon monoxide, halogens and isocyanides as ligands. Recently, the self-assembled supramolecules with pentamethylcyclopentadienyl or cyclopentadienyl groups have been reported by several groups [3]. Recently, we have reported preparation of supramolecular complexes based on quasi-octahedral geometries of rhodium(III) and iridium(III) bearing pentamethylcyclopentadienyl ligand [4]. This type of complexes can lead to compounds with diverse dimensionality, in comparison with square planar complexes. Chemistry on interaction between dpmp and octahedral complexes has attracted our attention. In regard with supramolecules, we were interested in the preparation of polymetallic compounds bearing dpmp and pentamethylcyclopentadienyl (or arenes) ligands, in which the chemistry has not been developed yet. We report the preparation and stereochemistry of mono- and dinuclear complexes of rhodium(III), iridium(III) and ruthenium(II) bearing dpmp and pentamethylcyclopentadienyl ligands.

Reactions of [Cp*RhCl$_2$]$_2$ (**1a**) with dpmp in the presence of KPF$_6$ generated mono- and dinuclear complexes [Cp*RhCl(dpmp)](PF$_6$) (**2a**) [5] and [Cp$^*_2$Rh$_2$Cl$_3$(dpmp)](PF$_6$) (**3a**) [5], respectively, depending on the reaction conditions (Scheme 1). Each of these

---

* Corresponding author. Tel.: +81-474-72-5076; fax: +81-474-75-1855.

E-mail addresses: yamamoto@chem.sci.toho-u.ac.jp (Y. Yamamoto), i45100a@nucc.cc.nagoya-u.ac.jp (K. Tatsumi).

[1] Fax: +81-52-789-2943.

0022-328X/03/$ - see front matter © 2003 Elsevier Science B.V. All rights reserved.
doi:10.1016/S0022-328X(03)00096-2

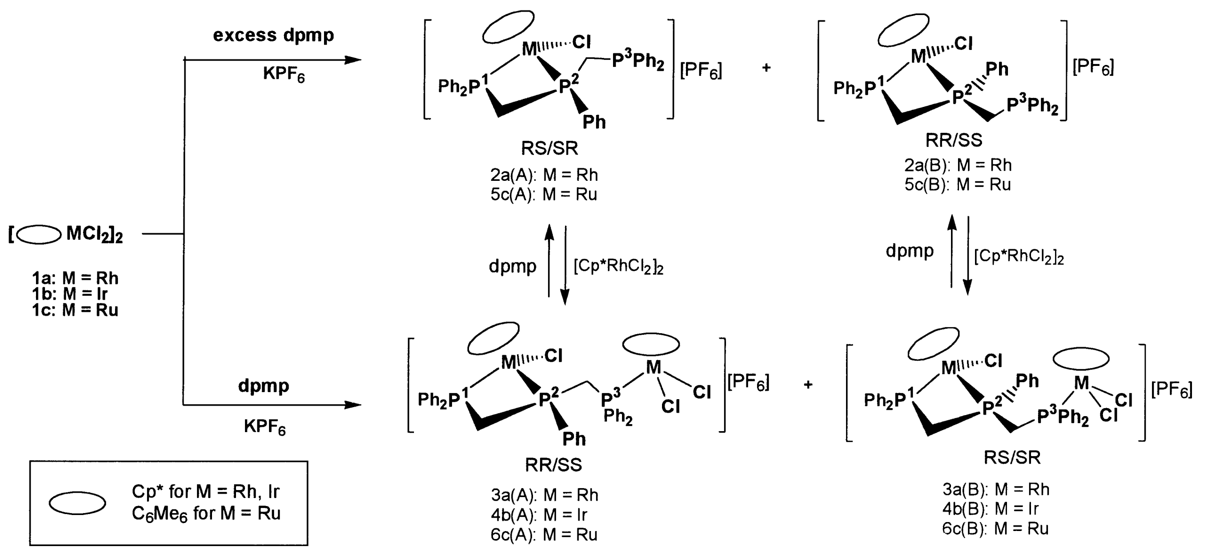

Scheme 1.

complexes consists of two sets of isomers (A and B) separated by successive recrystallization. On the basis of ^{1}H-NMR spectrum, the reaction mixture of **2a** consists of an intensity ratio of 2:1 for A:B. The ^{1}H-NMR spectrum of **2a**(**A**) showed a triplet at δ 1.74 for Cp* protons. The ^{31}P{^{1}H}-NMR spectrum showed three resonances at δ -24.3 (d, $^2J_{P3P2} = 81.0$ Hz, P^3), -9.84 (ddd, $^1J_{RhP2} = 118.0$ Hz, $^2J_{P2P1} = 105.0$ Hz, $^2J_{P2P3} = 81.0$ Hz, P^2) and -3.11 (dd, $^1J_{P1Rh} = 115.5$ Hz, $^2J_{P1P2} = 105.0$ Hz, P^1) for the dpmp ligand. The ^{1}H-NMR spectrum of **2a**(**B**) showed a triplet at δ 1.78 for Cp* protons. The ^{31}P{^{1}H}-NMR spectrum showed three resonances at δ -31.1 (d, $^2J_{P3P2} = 42.0$ Hz, P^3), -9.93 (ddd, $^1J_{RhP2} = 112.5$ Hz, $^2J_{P2P1} = 100.0$ Hz, $^2J_{P2P3} = 42.0$ Hz, P^2) and -5.00 (dd, $^1J_{P1Rh} = 116.5$ Hz, $^2J_{P1P2} = 100.0$ Hz, P^1). The X-ray analysis of **2a**(**A**) revealed that an Rh atom is connected by terminal and central P atoms and another P atom is free (Fig. 1) [6]. This molecule has two chiral centers. Since the priority order of the ligands is Cp* > Cl > P^1 > P^2 for the Rh center and Rh > Ph > C^1 > C^2 for the central P^2 atom, where C^1 and C^2 is the methylene carbon atoms between P^1 and P^2 atoms and between P^2 and P^3 atoms, respectively, complex **2a**(**A**) is an $R_{Rh}S_P$–$S_{Rh}R_P$ pair. Thus **2a**(**B**) is assumed to be an $R_{Rh}R_P$–$S_{Rh}S_P$ pair.

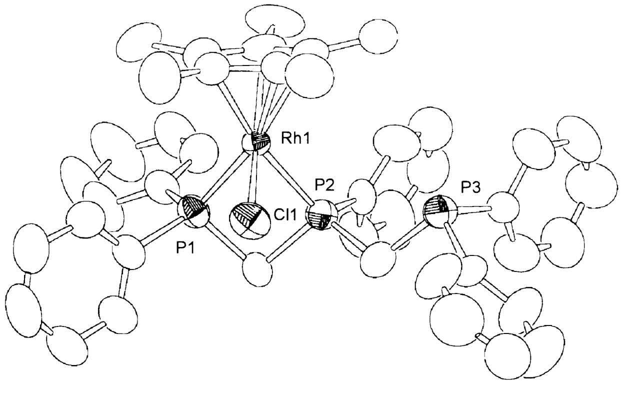

Fig. 1. Molecular structure of **2a**(**A**). A PF_6 was omitted for clarity. Selected bond lengths (Å) and angles (°): Rh(1)–Cl(1), 2.389(3); Rh(1)–P(1), 2.303(3); Rh(1)–P(2), 2.338(3); Cl(1)–Rh(1)–P(1), 83.9(1); Cl(1)–Rh(1)–P(2), 85.0(1); P(1)–Rh(1)–P(2), 71.6(1).

Complex **3a** consists of a population of 1.1:1.0 for **3a**(**A**) and **3a**(**B**). The ^{1}H-NMR spectrum of **3a**(**A**) showed a doublet at δ 1.28 and a triplet at δ 1.55 for Cp* protons. The ^{31}P{^{1}H}-NMR spectrum showed three resonances at δ -10.0 (dt, $^1J_{Rh1P2} = {}^2J_{P2P1} = 104.5$ Hz, $^2J_{P2P3} = 55.0$ Hz, P^2), -2.57 (dd, $^1J_{P1Rh1} = 114.5$ Hz, and $^2J_{P1P2} = 104.5$ Hz, P^1) and -28.1 (dd, $^1J_{P3Rh2} = 144.5$ Hz, $^2J_{P3P2} = 55.0$ Hz, P^3). The ^{1}H-NMR spectrum of **3a**(**B**) showed a doublet at δ 1.27 and a triplet at δ 1.73 for Cp* protons. The ^{31}P{^{1}H}-NMR spectrum showed three resonances at δ -13.3 (ddd, $^1J_{P2Rh} = 110.5$ Hz, $^2J_{P2P1} = 105.5$ Hz, $^2J_{P2P3} = 53.5$ Hz, P^2), -10.1 (dd, $^1J_{P1Rh} = 115.5$ Hz, $^2J_{P1P2} = 105.5$ Hz, P^1) and -30.1 (dd, $^1J_{P3Rh} = 145.0$ Hz, $^2J_{P3P2} = 53.5$ Hz, P^3). The X-ray analysis of **3a**(**B**) revealed that an Rh atom is connected by terminal and central P atoms and another Rh atom is coordinated to another terminal P atom (Fig. 2) [7]. This molecule has two chiral centers. Since the priority order of the ligands is Cp* > Cl > P^1 > P^2 for the Rh center and Rh > Ph > C^2 > C^1 for the central P^2 atom, complex **3a**(**B**) is an $R_{Rh}S_P$–$S_{Rh}R_P$ pair. Thus **3a**(**A**) is an $R_{Rh}R_P$–$S_{Rh}S_P$ pair. The geometries around Rh and P^2 atoms were found to be similar for **2a**(**A**) and **3a**(**A**), and for **2a**(**B**) and **3a**(**B**). No isomerization from **2a**(**A**) (**3a**(**A**)) to **2a**(**B**) (**3a**(**B**)) and its reverse reaction occurred at room temperature. No reaction of **2a**(**A**) with xylyl isocyanide occurred.

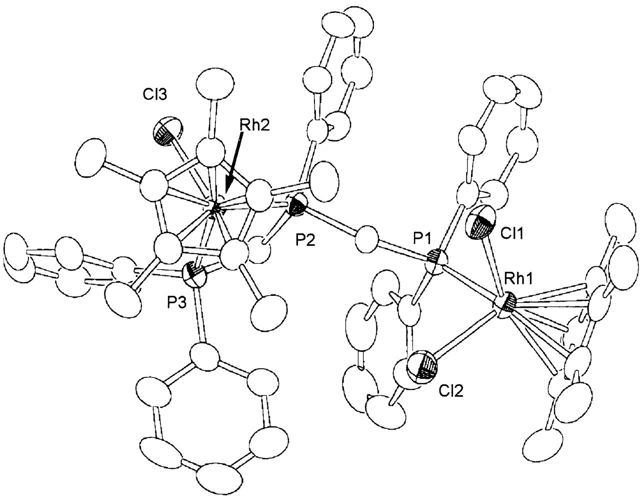

Fig. 2. Molecular structure of **3a**(**B**). A PF_6 anion was omitted for clarity. Selected bond lengths (Å) and angles (°): Rh(1)–Cl(1), 2.420(2); Rh(1)–Cl(2), 2.425; Rh(1)–P(1), 2.335(2); Rh(2)–Cl(3), 2.375(2); Rh(2)–P(2), 2.314(2); Rh(2)–P(3), 2.305(2); Cl(1)–Rh(1)–Cl(2), 91.67(7); Cl(1)–Rh(1)–P(1), 88.64(5); Cl(2)–Rh(1)–P(1), 89.93(6); Rh(1)–P(1)–C(51), 106.9(2); P(1)–C(51)–P(2), 129.9(3); Cl(3)–Rh(2)–P(2), 86.02(5); Cl(3)–Rh(2)–P(3), 86.58(6); P(2)–Rh(2)–P(3), 72.28(5); Rh(2)–P(3)–C(52), 95.1(2); P(2)–C(52)–P(3), 95.783; Rh(2)–P(2)–C(52), 94.8(2).

Complex **2a**(**A**) or **2a**(**B**) was treated with **1a** at room temperature, exclusively generating **3a**(**A**) or **3a**(**B**), respectively. Complex **3a**(**A**) or **3a**(**B**) was treated with dpmp in a similar way, affording **2a**(**A**) or **2a**(**B**), respectively. In these reactions, the conversion from **2a**(**B**) to **3a**(**B**) and its reverse reaction are slower than inter-conversion between **2a**(**A**) and **3a**(**A**). These reactions proceeded stereospecifically.

When $[Cp^*IrCl_2]_2$ (**1b**) reacted with dpmp in the presence of KPF_6, isolable complexes were orange (**4b**(**A**)) and yellow (**4b**(**B**)) ones having the formula of $[Cp^*_2Ir_2Cl_3(dpmp)](PF_6)$ under various reaction conditions, without producing any mono-nuclear complexes [5]. Population of **4b**(**A**) and **4b**(**B**) is 1:1.1. In the ^{1}H-NMR spectra, Cp* protons showed a doublet at δ 1.27 and a triplet at δ 1.56 for **4b**(**A**) and a doublet at δ 1.27 and a triplet at δ 1.79 for **4b**(**B**). No isomerization was observed standing for 120 h, whereas the treatment of **4b**(**B**) with xylyl isocyanide led to an isomerization to **4b**(**A**), almost quantitatively, suggesting that **4b**(**A**) is superior in stability to **4b**(**B**) (Eq. (1)). Metallacycle containing the Rh atom showed to be more stable than that containing the Ir atom.

$$\mathbf{4b(B)}\rightarrow\mathbf{4b(A)} \tag{1}$$

The X-ray analysis of **4b**(**A**) revealed that the structure is essentially similar to that of rhodium analog **3a**(**B**), and the difference is whether each of Cl atom and P^2-phenyl group is located on the opposite side for the former or on the same side for the latter. The molecular structure of **4b**(**A**) is depicted in Fig. 3 [8].

Reaction of $[(C_6Me_6)RuCl_2]_2$ (**1c**) with dpmp was carried out in the presence of KPF_6, generating mono- and dinuclear complexes $[(C_6Me_6)RuCl(dpmp)](PF_6)$ (**5c**) and $[(C_6Me_6)_2Ru_2Cl_3(dpmp)](PF_6)$ (**6c**), respectively, depending on reaction conditions [5]. These complexes consist of two diastereomers and the population is 2:1 for **5c**(**A**):**5c**(**B**) and 1:1.3 for **6c**(**A**):**6c**(**B**). In the ^{1}H-NMR spectra, the methyl protons appeared at δ 1.94 for **5c**(**A**) and at δ 2.06 for **5c**(**B**). X-ray analysis of **5c**(**A**) revealed to be a similar geometry to **2a**(**A**). The ^{1}H-NMR spectrum of **6c**(**A**) showed two singlets at δ 1.63 and 1.97 for methyl protons. The $^{31}P\{^1H\}$-NMR spectrum showed three resonances at δ −5.41 (dd, $^2J_{P2P1} = 50.0$ Hz, $^2J_{P2P3} = 92.0$ Hz, P^2), −0.07 (d,

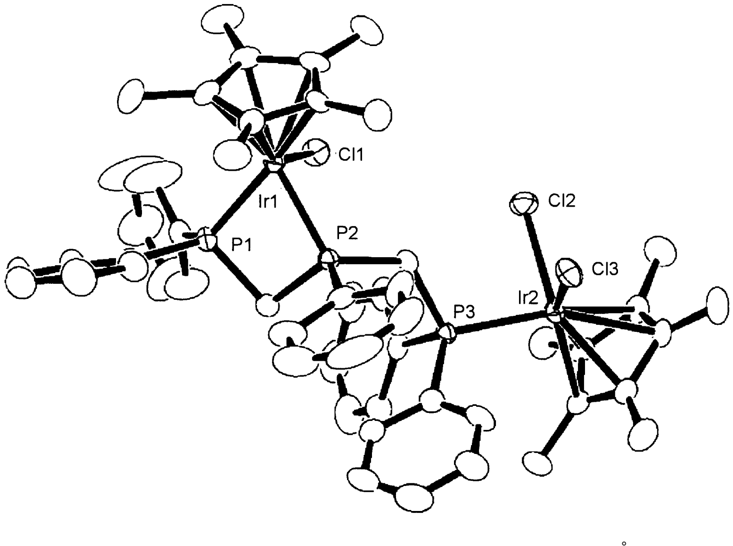

Fig. 3. Molecular structure of **4b**(**A**). The PF_6 anions were omitted for clarity. Selected bond lengths (Å) and angles (°): Ir(1)–Cl(1), 2.389(3); Ir(1)–P(1), 2.299(3); Ir(1)–P(2), 2.318(3); Ir(2)–Cl(2), 2.408(3); Ir(2)–Cl(3), 2.430(4); Ir(2)–P(3), 2.311; Cl(1)–Ir(1)–P(1), 85.7(1); Cl(1)–Ir(1)–P(2), 87.6(1); P(1)–Ir(1)–P(2), 72.2(1); Cl(2)–Ir(2)–Cl(3), 89.0(1); Cl(2)–Ir(2)–P(3), 88.9(1).

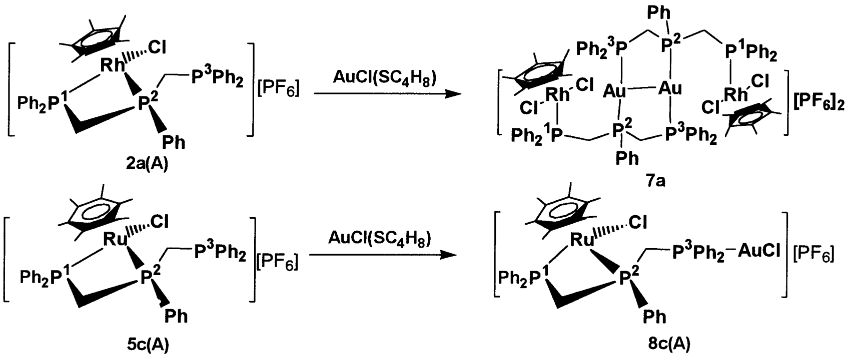

Scheme 2.

$^{2}J_{P3P2} = 92.0$ Hz, P^1) and −29.3 (d, $^{2}J_{P1P2} = 50.0$ Hz, P^3) for the dpmp ligand. The ^{1}H-NMR spectrum of **6c**(**B**) showed two singlets at δ 1.63 and 1.82 for methyl protons. The ^{31}P{^{1}H}-NMR spectrum showed three resonances at δ −0.49 (dd, $^{2}J_{P2P1} = 88.5$ Hz, $^{2}J_{P2P3} = 50.0$ Hz, P^2), −2.16 (d, $^{2}J_{P1P2} = 88.5$ Hz, P^1) and −27.1 (d, $^{2}J_{P3P2} = 50.0$ Hz, P^3). No isomerization proceeded in the absence and presence of xylyl isocyanide, suggesting the strong Ru–P bond.

Reactions of **2a**(**A**) or **5c**(**A**) with AuCl(C_4H_8S) were carried out, generating [{Cp*RhCl$_2$(dpmp)Au}$_2$](PF$_6$)$_2$ (**7a**) or [(C_6Me_6)RuCl(dpmp)AuCl](PF$_6$) (**8c**(**A**)), respectively (Scheme 2) [5]. X-ray analysis of **7a** revealed that the molecule has a crystallographically imposed inversion center in the middle of the Au···Au* vector (Fig. 4) [9]. Although an Au···Au separation of 3.203(2) Å is slightly long in comparison with those of 2.95–3.15 Å found for complexes bearing Au–Au bonds [10–12], the weak interaction between two Au atoms is assumed to be present. Each Cp*RhCl$_2$ moiety is connected by an outer P^1 atom of the dpmp ligand. The molecule also has two chiral centers of P2 and P2*, with an $R_{P2}S_{P2*}$–$S_{P2}R_{P2*}$ pair. It was confirmed by the X-ray analysis of **8c**(**A**) that the AuCl group coordinated to the free terminal P atom of **2a**(**A**) and its stereochemistry was remained to be an RR–SS pair [13].

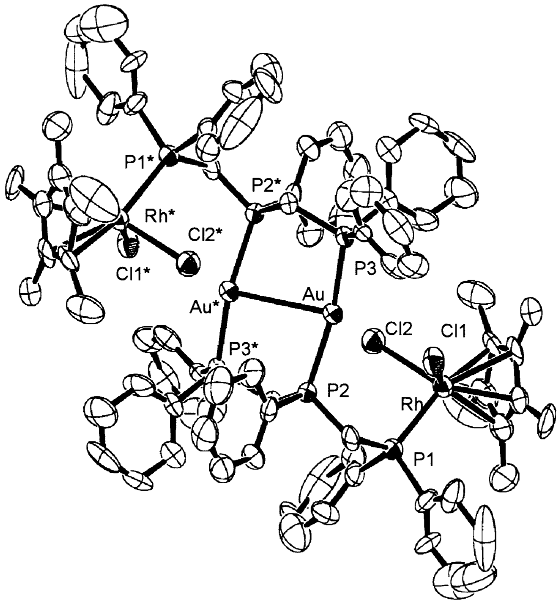

Fig. 4. Molecular structure of **7a**. The PF$_6$ anions were omitted for clarity. Selected bond lengths (Å) and angles (°): Au–P(2), 2.336(4); Au–P(3), 2.297(4); Rh–Cl(1), 2.432(5); Rh–Cl(2), 2.417(3); Rh–P(1), 2.326(4); P(2)–Au–P(3), 164.6(1); Cl(1)–Rh–Cl(2), 91.8(2); Cl(1)Rh–P(1), 87.3(2); Cl(2)–Rh(1)–P(1), 88.1(2).

The research on the mechanism and reactions of those complexes is now in progress.

1. Supplementary materials

Spectral data and elementary analyses for all new compounds, an ORTEP of **8c**(**A**), and X-ray analyses data (anisotropic thermal parameters, bond lengths and bond angles) for **2a**(**A**), **3a**(**B**), **4b**(**A**), **7a** and **8c**(**A**) are available. The CCDC numbers of these complexes are 190354, 190353, 202043, 190356 and 202044 for **2a**(**A**), **3a**(**B**), **4b**(**A**), **7a** and **8c**(**A**).

References

[1] A.P. Balch, in: L.H. Pignolet (Ed.), Homogeneous Catalysis with Metal Phosphine Complexes, Plenum Press, New York, 1983, p. 167 and references therein.

[2] T. Tanase, Y. Yamamoto, Trends Organomet. Chem. 3 (1999) 35 and references therein.

[3] (a) K.K. Klausmeyer, T.B. Rauchfuss, S.R. Wilson, Angew. Chem. 110 (1808) 1998;
(b) K.K. Klausmeyer, T.B. Rauchfuss, S.R. Wilson, Angew. Chem. Int. Ed. 37 (1998) 1694;
(c) S.M. Contakes, K.K. Klausmeyer, R.M. Milberg, S.R. Wilson, T.B. Rauchfuss, Organometallics 17 (1998) 3633;
(d) D.J. Darensbourg, W.-Z. Lee, M.J. Adams, D.L. Larkins, J.H. Reibenspies, Inorg. Chem. 38 (1999) 1378;
(e) S.M. Contakes, K.K. Klausmeyer, T.B. Rauchfuss, Inorg. Chem. 39 (2000) 2069.

[4] (a) H. Suzuki, N. Tajima, K. Tatsumi, Y. Yamamoto, Chem. Commun. (2000) 1801.;
(b) Y. Yamamoto, H. Suzuki, N. Tajima, K. Tatsumi, Chem. Eur. J. 8 (2002) 372.

[5] All new complexes were identified by their elemental analyses and spectroscopic data, which are reported in supplementary materials.

[6] Crystal data for **2a**(**A**): $C_{42}H_{44}P_4ClF_6Rh$, monoclinic, space group $P2_1/n$ (no. 14), $a = 12.487(4)$ Å, $b = 22.640(5)$ Å, $c = 15.395(6)$ Å, $\beta = 103.74(2)^\circ$, $V = 4227(2)$ Å^3, $Z = 4$, $\rho_{calc} = 1.453$ g cm^{-3}, $R = 0.155$, $R_w = 0.207$ [$w = 1/\sigma^2(F_o)$] for 7404 reflections with 482 variables and $R_1 = 0.074$ for 4155 reflections [$I > 2.0\sigma(I)$]. The measurement was made by Rigaku AFC5S. The structure was solved by Patterson methods (DIRDIF92) and refined by full-matrix least-squares techniques using the TEXSAN program package [14].

[7] Crystal data for **3a**(**B**): $C_{53}H_{61}P_4Cl_5F_6Rh_2$, monoclinic, space group $P2_1/c$ (no. 14), $a = 11.518(2)$ Å, $b = 25.566(2)$ Å, $c = 19.254(4)$ Å, $\beta = 94.95(2)^\circ$, $V = 5648(1)$ Å^3, $Z = 4$, $\rho_{calc} = 1.478$ g cm^{-3}, $R = 0.088$, $R_w = 0.134$ [$w = 1/\sigma^2(F_o)$] for 9939 reflections with 631 variables and $R_1 = 0.045$ for 6391 reflections [$I > 2.0\sigma(I)$]. The measurement was made by QuantumCCD/Rigaku AFC7 at 20°. The structure was solved by Patterson methods (DIRDIF92) and refined by full-matrix least-squares techniques using the TEXSAN program package [14].

[8] Crystal data for **4b**(**A**): $C_{52}H_{59}P_4Cl_3F_6Ir_2$, monoclinic, space group $P2_1/c$ (no. 14), $a = 15.367(2)$ Å, $b = 12.1256(5)$ Å, $c = 28.1703(9)$ Å, $\beta = 94.345(2)^\circ$, $V = 5233.9(6)$ Å^3, $Z = 4$, $\rho_{calc} = 1.793$ g cm^{-3}, $R = 0.052$ and $R_w = 0.098$ [$w = 1/\sigma^2(F_o)$] for 8913 reflections [$I > 3.0\sigma(I)$] with 604 variables. The measurement was made by QuantumCCD/Rigaku AFC7 at 20°. The structure was solved by Patterson methods and refined by full-matrix least-squares techniques using the TEXSAN program package [14].

[9] Crystal data for **7a**: $C_{84}H_{88}P_8Cl_4F_{12}Au_2Rh_2CH_2Cl_2$, monoclinic, space group $P2_1/n$ (no. 14), $a = 13.430(6)$ Å, $b = 13.59(1)$ Å, $c = 24.670(5)$ Å, $\beta = 95.53(3)^\circ$, $V = 4480(3)$ Å^3, $Z = 2$, $\rho_{calc} = 1.716$ g cm^{-3}, $R = 0.065$ and $R_w = 0.106$ [$w = 1/\sigma^2(F_o)$] for 4487 reflections [$I > 2.0\sigma(I)$] with 505 variables at 27°. The structure was solved by Patterson methods and refined by full-matrix least-squares techniques using the TEXSAN program package [14].

[10] A.L. Balch, V.J. Catalano, B.C. Noll, M.M. Olmstead, J. Am. Chem. Soc. 112 (1990) 7558.

[11] A.L. Balch, E.Y. Fung, M.M. Olmstead, J. Am. Chem. Soc. 112 (1990) 5181.

[12] H. Schmidbauer, A. Wohlleben, U. Schubert, A. Frank, G. Huttner, Chem. Ber. 110 (1977) 2751.

[13] Crystal data for **8c**(**A**): $C_{45}H_{49}Cl_8P_4F_6OAuRu$, $M = 1283.6$, monoclinic, space group $C2/c$ (no. 15), $a = 22.123(3)$ Å, $b = 12.8859(4)$ Å, $c = 35.639(1)$ Å, $\beta = 110.663(2)^\circ$, $V = 9506(1)$ Å^3, $Z = 8$, $D = 1.794$ g cm^{-3}, $\mu = 38.30$ cm^{-1} (Mo–K$_\alpha$), $F(0\,0\,0) = 5056$ and $T = 293$ K. Data were collected on a MSC/ADSC QuantumCCD/Rigaku AFC7. The structure was solved by direct methods and non-hydrogen atoms were refined anisotropically using full-matrix least-squares based on F to give $R_1 = 0.046$ and $R_w = 0.073$ for 7619 reflections. The ORTEP appears in the supplementary materials. The structure was solved by Patterson methods and refined by full-matrix least-squares techniques using the TEXSAN program package [14].

[14] TEXSAN: Crystal Structure Analysis Package, Molecular Structure Corporation Houston, TX, 1985 and 1992.